pISSN 2384-1095
eISSN 2384-1109

iMRI 2022;26:48-54

https://doi.org/10.13104/imri.2022.26.1.48

iMRI
Investigative Magnetic Resonance Imaging

Multifocal Extranodal Involvement in Diffuse Large B-cell Lymphoma (DLBCL): Bone, Soft tissue, Testis, and Kidney

Jae Sung Cho[1], Kyung Ryeol Lee[1], Bong Soo Kim[1], Guk Myung Choi[1], Jeong Sub Lee[1], Jung Sik Huh[2], Bogun Jang[3]

[1]Department of Radiology, Jeju National University Hospital, Jeju-si, Korea
[2]Department of Urology, Jeju National University Hospital, Jeju-si, Korea
[3]Department of Pathology, Jeju National University Hospital, Jeju-si, Korea

Case Report

Received: July 30, 2021
Revised: October 14, 2021
Accepted: October 14, 2021

Correspondence to:
Kyung Ryeol Lee, M.D., Ph.D.
Department of Radiology, Jeju National University Hospital, Aran 13 gil 15, Jeju Special Self-Governing Province, Jeju-si 63241, Korea.
Tel. +82-64-717-1373
Fax. +82-64-717-1377
E-mail: we1977@naver.com

This case report was approved by the relevant Institutional Review Board (IRB file no. 2021-05-017).

This is an Open Access article distributed under the terms of the Creative Commons Attribution Non-Commercial License (http://creativecommons.org/licenses/by-nc/4.0/) which permits unrestricted non-commercial use, distribution, and reproduction in any medium, provided the original work is properly cited.

Copyright © 2022 Korean Society of Magnetic Resonance in Medicine (KSMRM)

In this report we present a case of disseminated diffuse large B-cell lymphoma (DLBCL) in a 79-year-old man affecting the bone, soft tissue, testis, and both kidneys, which are rarely affected sites. The formation of a large mass in the bone, soft tissue, and testis due to DLBCL is rarely seen nowadays. In this article, we describe the imaging findings and clinical significance of multifocal extranodal involvement in DLBCL, focusing on involvement of bone, soft tissue, and testis.

Keywords: Non-Hodgkin lymphoma; Diffuse large B-cell lymphoma; Extranodal; Bone; Soft tissue, Testis

INTRODUCTION

Diffuse large B-cell lymphoma (DLBCL) is the most common histologic subtype of non-Hodgkin's lymphoma (NHL), accounting for approximately 25% of all NHLs and is predominant in older individuals (median age, 64 years) (1). Most DLBCLs originate from lymph nodes or other lymphatic tissues, such as the spleen, Waldeyer's ring, or thymus. However, 30% of cases initially present at extranodal sites. Secondary non-lymphoid organ involvement of lymphoma is more common than is primary extranodal lymphoma. One previous study showed that the incidence of extranodal sites in DLBCL were bone (7%); soft tissue (4.8%); skin (1.1%); testis (0.6%); and kidney (1.6%) (1).

The patient in this case had multifocal extranodal DLBCL with minimal lymph-node involvement, affecting the muscle, bone, testis, and both kidneys, which are rarely affected organs. At present, an advanced disease with large masses is rarely experienced in daily routine practice, because most lymphomas are diagnosed early. Our objective in this case report is to illustrate imaging findings of multiorgan involvement in DLBCL that formed a huge mass with musculoskeletal and testicular involvement, and to assess the advantage of MRI over that of positron-emission tomography (PET)-CT or CT.

CASE REPORT

A 79-year-old man presented with a three-month history of persistent pain and swelling in his right lower leg. Without proper medical investigation or treatment, he also experienced progressive painful swelling of the scrotum. Therefore, he visited the urology department of the Jeju National University Hospital. He had a huge firm soft-tissue mass in the left scrotum and an asymmetrically enlarged right leg on physical examination. The patient had no history of trauma or cancer nor any reported history of fever, night sweats, unexplained weight loss, or other constitutional symptoms. His initial lactate dehydrogenase level (417 IU/L) was elevated, whereas other laboratory findings were within normal limits. His Eastern Cooperative Oncology Group (ECOG) performance status was 2.

We did plain radiography, CT, and MRI to evaluate the mass in the right lower leg. Plain radiographs revealed a soft-tissue density lesion with a lobulated margin in the mid-to-distal portion of the right lower leg. There was irregular osteolytic bone destruction in the diaphysis of the right fibula, adjacent to the soft-tissue density lesion (Fig. 1). We considered malignant bone or soft-tissue tumors based on the plain radiograph findings. MRI revealed a large, irregular soft-tissue mass in the right lower leg, measuring 22.2 cm in diameter (Fig. 2). The extraosseous portion of the mass showed an infiltrative soft-tissue tumor extending to the muscles of the anterior, lateral, and deep posterior compartments of the right lower leg and to the subcutaneous fat and skin of the lower leg. The mass showed preserved muscle architecture, such as intermuscular fascia and fat planes, with the presence of intramuscular traversing vessels, homogeneous high signal intensity on T2-weighted images, and a homogeneous signal intensity on T1-weighted images slightly higher than that of skeletal muscle. The mass showed relatively homogeneous enhancement; we considered some poorly enhancing portions within the mass to be necrotic tissue. The osseous portion of the mass corresponding to the plain radiograph revealed an infiltrative tumor, replacing the normal bone marrow with cortical destruction at the anterior aspect of the diaphysis of the right fibula.

a b

Fig. 1. Anteroposterior (a) and lateral (b) radiographs of the right lower leg revealed a soft-tissue lesion (arrows) with irregular osteolytic bone destruction (arrowheads) in the diaphysis of the right fibula.

We initially did US to evaluate the left scrotal mass (Fig. 3). A huge heterogeneously hypoechoic mass encased the left testis, epididymis, and spermatic cord and extended to the inguinal canal along the spermatic cord. It also displayed increased vascularity on color Doppler US. Scrotal MRI revealed an approximately 13.8-cm heterogeneously enhancing mass with small internal necrotic or cystic portions in the left scrotum (Fig. 3). The mass showed preserved internal vascular and ductal structures without luminal narrowing or occlusion and showed markedly restricted diffusion on diffusion-weighted images (DWI).

Enhanced abdominal-lower extremity CT additionally revealed multiple enhancing soft-tissue lesions in both kidneys, the left perinephric space, and right hip area. These lesions showed homogeneous enhancement with an infiltrative nature. Only a few enlarged lymph nodes were distinguishable in the left external iliac area. The enhanced CT findings of the masses in the right lower leg and left scrotum were similar to those on the MRI: large soft-tissue masses with heterogeneous enhancement and some necrotic portions. Additionally, non-enhanced chest CT revealed homogeneous soft-tissue lesions in the subglottic to upper paratracheal area of the left lower neck and right shoulder area. We also detected focal consolidative lesions in the upper and lower lobes of the right lung. PET-CT demonstrated increased uptake of ^{18}F-fluorodeoxyglucose (FDG) in the previously described sites, including the left lower neck, right lung, both kidneys, left scrotum, and right lower leg. Additionally, PET-CT revealed a focal FDG hot uptake lesion at the arc of the right fourth rib (Fig. 4).

Two large masses in the right calf and left testis appeared as soft-tissue masses with relatively well-preserved organ architecture and the presence of traversing vessels. Therefore, we first considered lymphoma as the diagnosis.

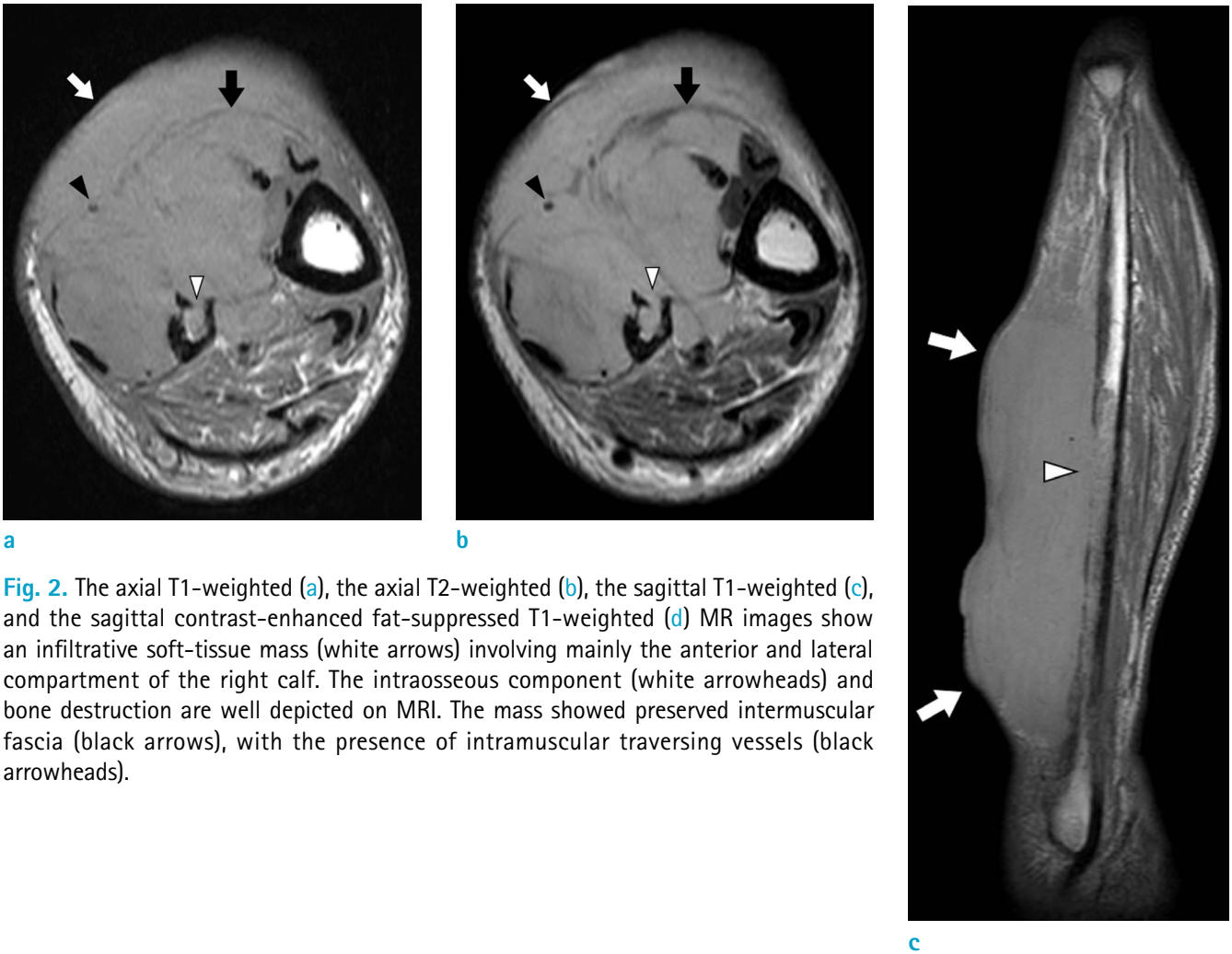

a b c

Fig. 2. The axial T1-weighted (a), the axial T2-weighted (b), the sagittal T1-weighted (c), and the sagittal contrast-enhanced fat-suppressed T1-weighted (d) MR images show an infiltrative soft-tissue mass (white arrows) involving mainly the anterior and lateral compartment of the right calf. The intraosseous component (white arrowheads) and bone destruction are well depicted on MRI. The mass showed preserved intermuscular fascia (black arrows), with the presence of intramuscular traversing vessels (black arrowheads).

Metastatic cancer usually shows more heterogeneous enhancement with necrotic portions and a lower tendency to preserve the fascia and vessels. We did a US-guided core-needle biopsy on the tumor in the right anterior tibialis muscle. Following the WHO classification of lymphomas (2008), we diagnosed it as malignant lymphoma, diffuse large B-cell type; the gene-expression profile was the germinal center B-cell-like (GCB) subtype. He was classified as advanced disease (stage IV) on the Lugano classification. The National Comprehensive Cancer Network - International Prognostic Index (NCCN-IPI) score was 6, which meant the high-risk prognostic group. The patient is currently being treated with chemotherapy (standard R-CHOP regimen) and is under observation. He achieved complete remission on PET-CT (Deauville scale 2) after three cycles of regimen.

a

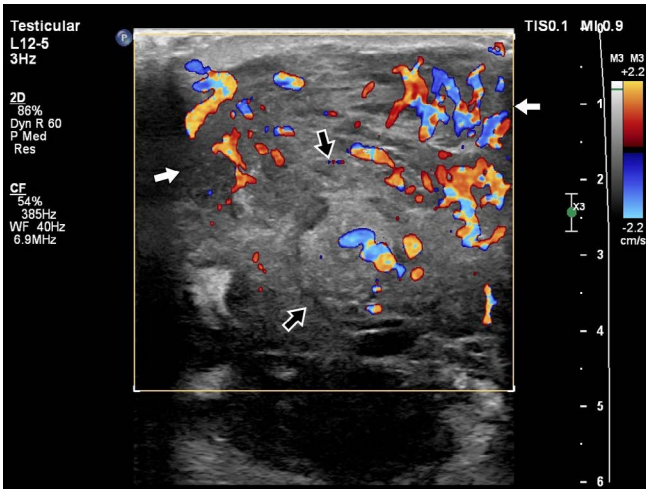

b

c

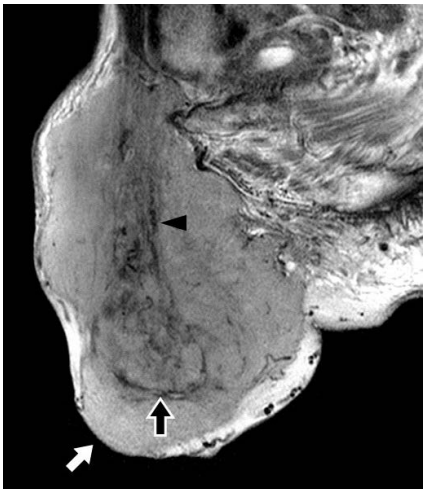

d

e

Fig. 3. US and MR images of the huge scrotal mass. Color Doppler US image (a) demonstrates a huge heterogeneously hypoechoic and hypervascular mass (white arrows) encasing the left testis (black arrows) and epididymis. The coronal T1-weighted MR image (b) and the sagittal T2-weighted MR image (c) demonstrates relatively heterogeneous signal intensity soft tissue mass (white arrows) encasing the left testis (black arrow), epididymis, and spermatic cord. Internal vascular and ductal structures show no definite luminal narrowing or occlusion (black arrowheads in b-f). The sagittal contrast-enhanced T1-weighted MR image (d) shows a slightly heterogeneously enhancing soft tissue mass (white arrow) with a small necrotic portion. The axial diffusion-weighted image (e) with a high b value (1000 s/mm^2) shows a high signal-intensity mass (white arrow) in the left scrotum.

Fig g에 대한 설명 추가하여 주세요.

f

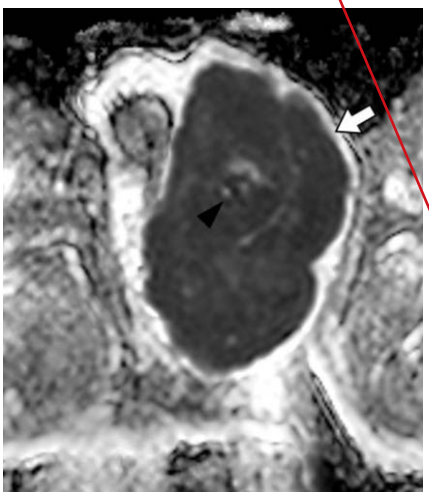

g

Fig. 3. The corresponding lesion (white arrow) has low value on the apparent diffusion coefficient map (f).

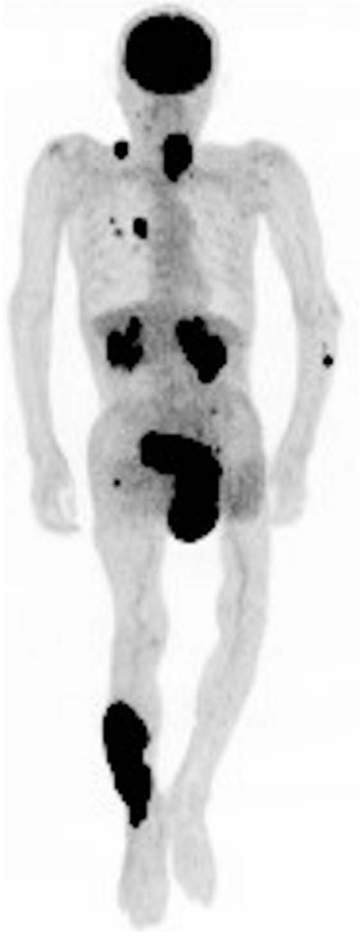

a

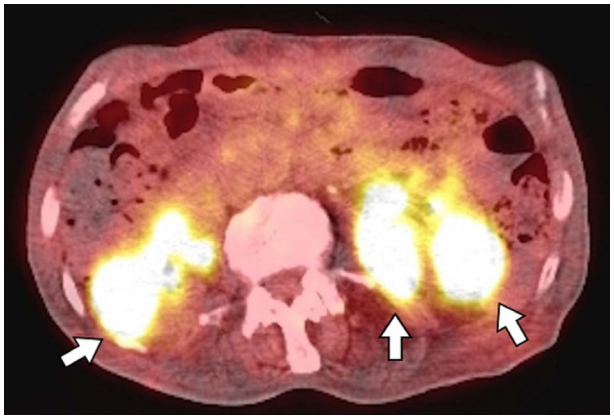

b

Fig. 4. PET-CT demonstrates increased uptake in the left subglottic to upper paratracheal region, right lower neck, right lung, right fourth rib, both kidneys, both adrenal glands, left scrotum, left external iliac lymph node, and around the right hip joint and right lower leg (a). The axial PET CT image at the level of the kidney showing multifocal ^{18}F-FDG hot uptake lesions in both kidneys (arrows) (b).

DISCUSSION

DLBCL is one of the most common lymphoid neoplasms, accounting for 33% of all NHL cases. Lugano staging is a recently developed system for staging and response assessment for Hodgkin's lymphoma and NHL in clinical practice (2). It integrates and simplifies the Ann Arbor stage, which is an anatomical description of the extent of lymphoma. The staging system is as follows:

involvement of one nodal station (stage I),

two or more nodal states on the same side (stage II)

or both sides of the diaphragm (stage III), and

diffuse or disseminated involvement of one or more extranodal organs or tissues (stage IV).

Stages I and II are classified as "limited disease," and stages III and IV are "advanced disease." Advanced and extranodal diseases, according to the Lugano classification, in NHL still carried a poor prognosis in the rituximab era (3). In the present case, the mass showed multifocal extranodal involvement and was stage IV lymphoma according to the Lugano classification. Therefore, we expected the prognosis in this case to be poor. However, because the standard R-CHOP regimen preferentially considered for germinal center B-cell type DLBCL was relatively effective in previous studies, diagnostic assessment and therapeutic response evaluation using imaging were very useful for proper management.

MRI plays an integral role in assessing lymphoma involving the musculoskeletal system and is very useful for visualizing soft-tissue masses and delineating associated osseous involvement. Muscular DLBCL may present as a focal mass or diffuse muscular infiltration in the presence of intramuscular traversing vessels and preserved muscle architecture, such as intermuscular fascia and fat planes (4). In the present case, the tumor extended to the fibula and involved the bone marrow. Secondary osseous lymphoma is more common than is primary osseous lymphoma, being detected in approximately 16% of patients with lymphoma and is usually due to NHL, with DLBCL being the most common type. The radiologic appearance of bone involvement in lymphoma can very. The most common appearance is the lytic-destructive pattern with a moth-eaten/permeative wide transition zone (5). Cortical destruction is often associated with the involvement of the adjacent muscle and soft tissue and can cause pathologic fractures. Bone-marrow involvement where tumors replace normal fatty marrow appears with a low intensity on T1-weighted images and with high intensity on T2-weighted images. We explained the musculoskeletal involvement in this case as bony involvement of muscular lymphoma rather than as muscular involvement of osseous lymphoma, because the extraosseous component was much larger than the osseous component.

Genitourinary lymphoma accounts for less than 5% of all extranodal NHL cases. The testis is uncommon as a site of extranodal involvement in DLBCL and is noted in approximately 1% of cases (1, 6). The majority (~80%) of cases of scrotal lymphoma are of DLBCL. Imaging studies reflect the infiltrative but nondestructive characteristics of lymphoma. In contrast to the presentation in most cases of non-lymphomatous testicular cancer, testicular lymphomas commonly involve the spermatic cord, epididymis, and vascular invasion, as seen in this case. Normal testicular tissues are replaced by tissues with low signal intensity on T1- and T2-weighted images, with low-level enhancement (less than that of the normal testicular tissue) (7). Primary testicular lymphoma has a marked tendency for systemic dissemination (6).

^{18}F-FDG PET-CT and contrast-enhanced CT are reference standards for staging lymphomas in the Lugano classification (2). For this reason, a patient with lymphoma undergoes many rounds of PET-CT for staging, response assessment, and detection of recurrence. However, MRI can be the imaging modality of choice for pediatric and pregnant patients with DLBCL, because there are none of the risk associated with exposure to ionizing radiation. MRI provides high soft-tissue resolution and is the best imaging modality for the central nervous, musculoskeletal, and genitourinary systems. It can depict the exact extent of disease, provide more information about neurovascular or bone-marrow involvement, and can better differentiate lymphoma from other tumorous or non-tumorous conditions than can PET-CT. Whole-body MRI (WB-MRI) using DWI is a promising radiation-free imaging technique for lymphoma staging and treatment-response assessment. Because lymphomatous lesions have high cellularity and a high nucleus-to-cytoplasm ratio, they have low apparent diffusion coefficient (ADC) values on ADC maps. In patients with FDG-avid lymphoma, including DLBCL, diffusion-weighted WB-MRI has a sensitivity of 97% for disease staging and is only slightly inferior to PET-CT (8). WB-MRI as an imaging modality is less histologically dependent than is PET-CT, and provides better diagnoses than does PET-CT for indolent NHLs with low ^{18}F-FDG avidity and may be the imaging test of choice (9).

MRI is a very useful modality for evaluating extranodal

involvement in cases of lymphoma, especially in the musculoskeletal system and soft tissue (10). Image findings in this case well depict the characteristic imaging findings of lymphoma. MRI is also advantageous for tumor characterization and differentiation from other tumorous and non-tumorous conditions. Further, WB-MRI can better depict the extent of disease than can PET-CT. Thus, the use of MRI for evaluating lymphoma can be expanded in clinical practice.

REFERENCES

1. Takahashi H, Tomita N, Yokoyama M, et al. Prognostic impact of extranodal involvement in diffuse large B-cell lymphoma in the rituximab era. Cancer 2012;118:4166-4172
2. Cheson BD, Fisher RI, Barrington SF, et al. Recommendations for initial evaluation, staging, and response assessment of Hodgkin and non-Hodgkin lymphoma: the Lugano classification. J Clin Oncol 2014;32:3059-3068
3. Zhou Z, Sehn LH, Rademaker AW, et al. An enhanced International Prognostic Index (NCCN-IPI) for patients with diffuse large B-cell lymphoma treated in the rituximab era. Blood 2014;123:837-842
4. Chun CW, Jee WH, Park HJ, et al. MRI features of skeletal muscle lymphoma. AJR Am J Roentgenol 2010;195:1355-1360
5. Lim CY, Ong KO. Imaging of musculoskeletal lymphoma. Cancer Imaging 2013;13:448-457
6. Gundrum JD, Mathiason MA, Moore DB, Go RS. Primary testicular diffuse large B-cell lymphoma: a population-based study on the incidence, natural history, and survival comparison with primary nodal counterpart before and after the introduction of rituximab. J Clin Oncol 2009;27:5227-5232
7. Zicherman JM, Weissman D, Gribbin C, Epstein R. Best cases from the AFIP: primary diffuse large B-cell lymphoma of the epididymis and testis. Radiographics 2005;25:243-248
8. Mayerhoefer ME, Karanikas G, Kletter K, et al. Evaluation of diffusion-weighted MRI for pretherapeutic assessment and staging of lymphoma: results of a prospective study in 140 patients. Clin Cancer Res 2014;20:2984-2993
9. Wang D, Huo Y, Chen S, et al. Whole-body MRI versus (18)F-FDG PET/CT for pretherapeutic assessment and staging of lymphoma: a meta-analysis. Onco Targets Ther 2018;11:3597-3608
10. Kim SH. Collison tumor of adenocarcinoma and diffuse large B-cell lymphoma in the rectum: a case report and literature review. Investig Magn Reson Imaging 2019;23:374-380